doi:10.3788/gzxb20124108.0922

Structural, Optical and Electrical Properties of Chromium Thin Films Prepared by Magnetron Sputtering

LIN Jian-ping[1], LIN Li-mei[2], GUAN Gui-qing[1], WU Yang-wei[2], LAI Fa-chun[2]
(1 *Department of Physics and Electric Engineering, Ningde Normal University, Ningde, Fujian* 352100, *China*)
(2 *Department of Physics, Fujian Normal University, Fuzhou* 350108, *China*)

Abstract: Chromium (Cr) thin films with thickness ranging from 5 nm to 114 nm were deposited on quartz substrates by the direct current magnetron sputtering. X-ray diffraction and optical spectrophotometer were employed to characterize the crystal structure and optical properties, respectively. Based on the Drude optical dielectric model, optical constants and thicknesses of the films were calculated from the transmittance and reflectance data. The sheet resistance was measured by Van der Pauw method. The results show that the films have a body-centered cubic crystalline structure. The grain size of the film increases gradually and the crystalline performance enhances as film thickness increases. When film thickness is less than 32 nm, transmittance decreases sharply, reflectance and extinction coefficient increase rapidly as the increase of thickness. When thickness is larger than 32 nm, both refractive index and extinction coefficient decrease gradually until they become stable as the thickness increases. Resistivity is the first order exponential decay when thickness increases from 5 nm to 114 nm.

Key words: Magnetron sputtering; Cr film; Structure; Optical properties; Electrical properties
CLCN: O439 **Document Code**: A **Article ID**: 1004-4213(2012)08-0922-5

0 Introduction

Cr films have been used widely in engineering component, optical beam splitters, surface decoration, photomasks, and magnetic recording disks, because of their high hardness, well wear resistance, and corrosion resistance. For example, Cr-Ni films can be used as a resistor[1]. Cr films are used as the interlayer of magnetic multilayer films because they have a well adhesiveness with substrate[2]. They are also used as metallic coatings to increase the resistance to environmental degradation of less corrosion resistant metals or alloys[3]. Furthermore, Cr films can be used as a light absorbing layer in an optical interference display unit[4], flat-panel displays, spatial light modulators, and tunable filters[5]. Many deposition techniques have been used to prepare Cr thin films, such as thermal evaporation, electron beam evaporation[1,6-8] and magnetron sputtering[2-3,9-12]. Among these methods, magnetron sputtering is most common used because it has the advantages of reproducibility, stability, and high deposition rate[13].

It is well known that the structural, optical, and electrical properties of the film depend very much on the deposition condition and film thickness. For instance, Abari *et al.*[12] had studied the effect of Ar partial pressure on the microstructure and electrical properties of Cr films deposited by magnetron sputtering. Li *et al.*[9] found that the crystalline to amorphous structure transition of Cr film by the change of deposition rate. The effect of thickness on the structure and optical properties of Nb_2O_5 films had been investigated by Lai *et al.*[14]. Urban *et al.*[10] had studied the change of optical constant when Cr film thickness increases from 11.5 nm to 25.5 nm. Therefore, it is very necessary to study the optical and electrical properties of Cr film with different thicknesses for its application in optoelectronics.

In present study, we focus on the effect of thickness on the structural, optical, and electrical properties of Cr thin films prepared by direct current magnetron sputtering. Based on Drude optical dielectric model, refractive index,

Foundation item: The National Natural Science Foundation of China (No. 11074041) and the Science Foundation of Ningde Normal University (No. 2011H208)
First author: LIN Jian-ping (1965—), male, assistant professor, bacheler degree, mainly focuses on films material. Email: ndljp999@163.com
Received date: 2012-04-17 **Revised date**: 2012-06-11

extinction coefficient, and thickness of the film were calculated by transmittance and reflectance data.

1 Experimental details

Cr films were deposited by a direct current magnetron sputtering system on quartz substrates. A 99.99% pure Cr disc with a diameter of 60 mm and a thickness 5 mm was used as the target. The target-substrate distance was 60 mm. Quartz substrates, 1.0 mm thickness, 25 mm × 25 mm, were cleaned in acetone and ethanol several times before deposition. During the sputtering process, Ar flow rate controlled by a mass flow controller was 42.5 sccm. The base pressure of vacuum chamber was 4.0×10^{-4} Pa and the sputtering pressure was 1.1 Pa. The sputtering power was 60 W. Prior to depositing Cr films, the target was pre-sputtered for 2 min to remove its surface oxides. The films with different thicknesses were obtained by changing the deposition time from 10 s to 300 s.

The crystal structure of Cr films was examined by X-ray diffraction (XRD). An XRD study was carried out on an X′Pert PRO X-ray diffractometer with a high-intensity Cu Kα radiation ($\lambda = 1.540\ 6$ Å). In order to detect the small quantity microcrystalline, the incident X-ray beam was fixed at 0.5° angle to the sample surface. The normal incidence transmittance (T) and reflectance (R) were recorded by a double-beam spectrophotometer (UV-2450) in the wavelength range 200～900 nm. Sheet resistance and resistivity (ρ) were measured by Van der Pauw method.

In previous research, an optical model combining the Forouhi-Bloomer model with modified Drude model was given for determining the thickness and optical constants of indium tin oxide (ITO) films from the normal incidence transmittance data by Lai *et al*.[15], because ITO is a transparent conductive material. In this study, however, Cr is a metal, so we choose Drude model[16], which suits for metal material and is shown as

$$\varepsilon_r(\omega) = 1 - \frac{\omega_p}{\omega^2 + ir\omega} \tag{1}$$

where $\varepsilon_r(\omega)$ is relative dielectric constant, ω frequency, ω_p metal plasma frequency, and r damping coefficient. A computer program was written in FORTRAN for calculating the refractive index (n), extinction coefficient (k) and thickness (d) of Cr films by simulating the transmittance and reflectance data. A merit function for this calculation is defined as

$$f(d, n(\lambda), k(\lambda)) = \sum_{\lambda}[T_{meas}(\lambda) - T_{calc}(\lambda)]^2 + \sum_{\lambda}[R_{meas}(\lambda) - R_{calc}(\lambda)]^2 \tag{2}$$

where λ is wavelength, $T_{meas}(\lambda)$ and $R_{meas}(\lambda)$ refer to the measured transmittance and reflectance, respectively. $T_{calc}(\lambda)$ and $R_{calc}(\lambda)$ refer to the calculated transmittance and reflectance, respectively. The calculation process looks for proper d that minimizes the difference between the measured and calculated spectra, where the merit function has the minimum, so that the calculated spectrum is close to the measured spectrum to full extent. Moreover, the calculated film thickness was also confirmed by the measurement of a stylus profile (Newview 5000).

2 Result and discussion

2.1 Crystal structure

XRD patterns of Cr films with thickness ranging from 32 nm to 114 nm are shown in Fig. 1. There is no obvious diffraction peak in XRD pattern when $d = 32$ nm, However, for the other three samples, a peak at 44.3° appears and its intensity enhances with the increase of d. Comparing the diffraction peak position with the data from JCPDS international diffraction database (# 89-4055), this peak is (110) peak. It illustrates that Cr film is a body-centered cubic structure and has a preferred (110) orientation.

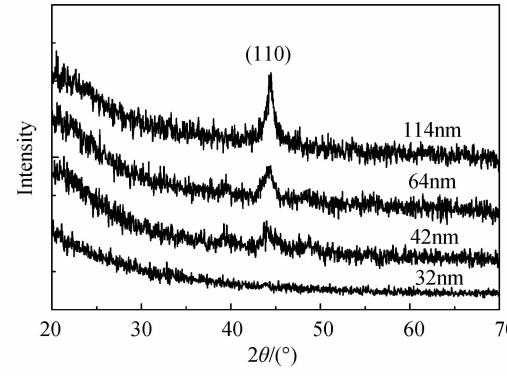

Fig. 1 XRD patterns of Cr films with different thicknesses

The mean grain size (d_g) of a film can be calculated by the Scherrer formula

$$d_g = 0.9\lambda/(B\cos\theta) \tag{3}$$

where θ, λ, and B are Bragg diffraction angle, X-ray wavelength, and full width at half maximum of diffraction peak, respectively. Therefore, d_g can be calculated from the data of XRD patterns. The mean grain sizes are 14.18 nm and 18.86 nm when thicknesses are 64 nm and 114 nm, respectively,

which illustrates that d_g increases with increasing thickness and the crystalline performance enhances.

2.2 Optical properties

The transmittance and reflectance of the films with different thicknesses are shown in Fig. 2. T in short wavelength is lower, and increases with the increase of wavelength. T at 700 nm wavelength is about 10% higher than T at 400 nm. The highest T of 5 nm thick film is closed to 80%. T decreases with the increase of d. When d increases from 5 nm to 32 nm, T sharply declines. T is lower than 10% as $d = 114$ nm, and is zero at ultraviolet spectral region. The number of free electron in film increases with the increase of d, which results in the enhancement of optical absorption and the decrease of T. When d reaches to a certain value, T is zero and will be no change with the increase of thickness.

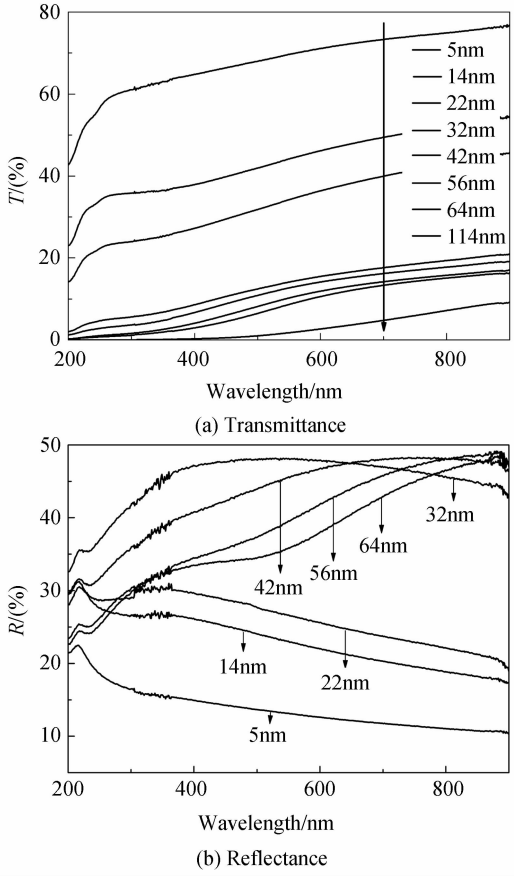

Fig. 2 Transmittance and reflectance of the films with different thicknesses

As seen in Fig. 2 (b), the variation of reflectance with different d is more complex than that of transmittance. When $d < 32$ nm, R enhances rapidly with the increase of d, which is consistent with the report by Bruce *et al*.[17]. The variation of R at 900 nm wavelength is relatively small when $d > 32$ nm. At ultraviolet and visible spectral regions, however, R decreases with the increase of d. In addition, in visible region, R is about 48% and its variation with wavelength is small as $d = 32$ nm.

Based on Drude optical dielectric model, d, refractive index (n), and extinction coefficient (k) of samples were calculated from the transmittance and reflectance data. Fig. 3 shows T and R of the samples with d of 32 nm and 64 nm. The solid lines are measured spectra and dotted lines are calculated spectra. As shown, the dotted line is consistent with the solid line, which illustrates that the calculated results are reliable.

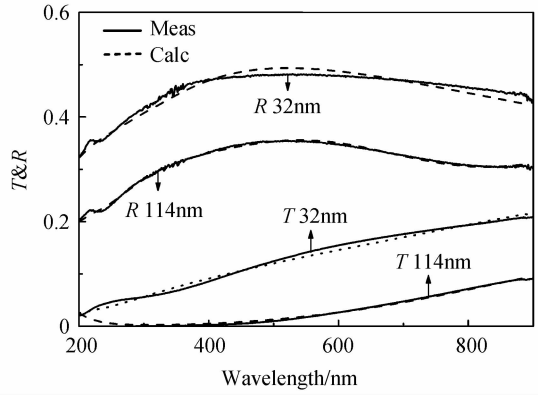

Fig. 3 Measured and calculated transmittance and reflectance of the films with thicknesses of 32 nm and 114 nm

Fig. 4 shows n and k of the films with different

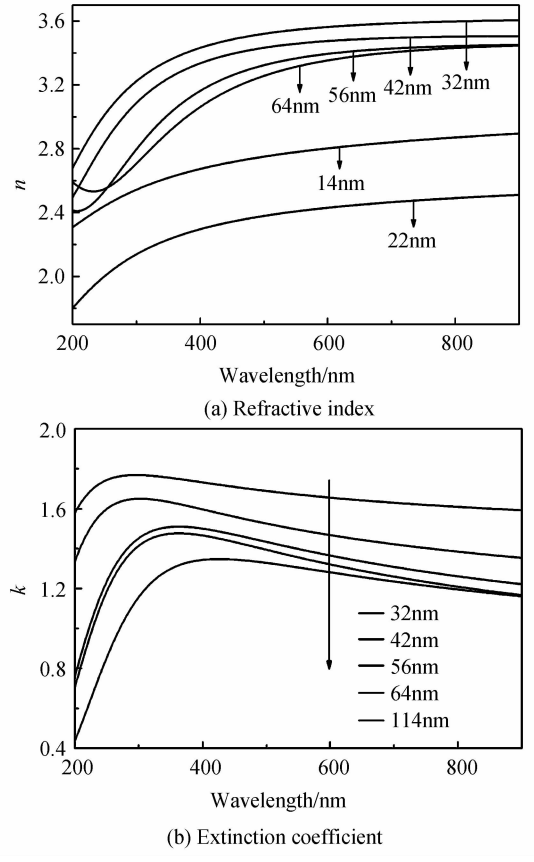

Fig. 4 Refractive index and extinction coefficient of the films

d as a function of wavelength. For the 64-nm thick sample, as the increase of λ, n decreases firstly and then increases, which is consistent with the report by Urban *et al*.[10]. k increases rapidly firstly and then declines gradually as λ increases.

The variation of n and k with thickness at $\lambda=$ 400 nm, 550 nm, and 800 nm is presented in Fig. 5. When d increases, n decreases sharply as $d<22$ nm, then increases rapidly as 22 nm$<d<$ 32 nm, and declines slowly as $d>32$ nm. As the increase of d, k enhances rapidly as $d<32$ nm, and then decreases slowly as $d>32$ nm.

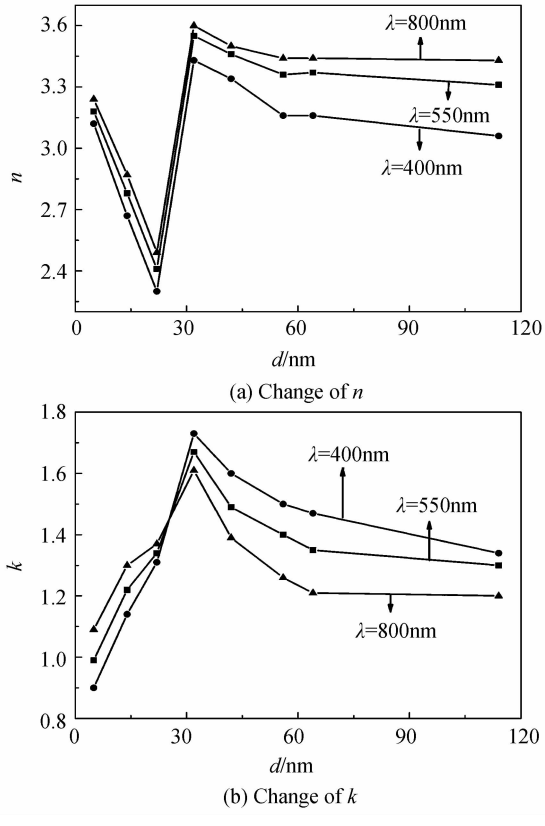

Fig. 5 Change of n and k with thickness at $\lambda=400$ nm, 550 nm, and 800 nm

The growth of a thin film starts with nucleation and formation of island. Three-dimensional film formation is the growth of islands until they touch one another to form a continuous network[18]. In the process of an island growth stage to a network stage, there are a lot of bare space on substrate, which results in a lower reflectance. As the film thickness increases, the film is more compact and enhances reflectivity. Therefore, for Cr film, when d increases from 5 nm to 32 nm, film structure converts from an island growth stage to a continuous network stage. So R and k increases, n decreases rapidly. When $d>32$ nm, the mean grain size in the film is larger than 12 nm and increases with the increase of thickness as can be seen in XRD results. The increase of grain size induces the enhancement of optical scattering, which results in the decrease of reflectance at ultraviolet and visible spectral regions, and the decline of n and k.

2.3 Electrical properties

The variation of resistivity is shown in Fig. 6. When $d=5$ nm, $\rho=47.8\ \Omega\cdot$cm and the uncertainty of resistivity ($\Delta\rho$) is 3.6 $\Omega\cdot$cm. As d increases to 14 nm, 64 nm, and 114 nm, ρ decreases to 17.1 $\Omega\cdot$cm, 11.8 $\Omega\cdot$cm, and 11.8 $\Omega\cdot$cm, and $\Delta\rho$ decreases to 1.2 $\Omega\cdot$cm, 0.1 $\Omega\cdot$cm, and 0.1 $\Omega\cdot$cm, respectively. When $d<5$ nm, film belongs to island structure and conductive electrons between islands are less, which results in a high ρ. When 5 nm$<d<$32 nm, film structure converts from an island growth stage to a network growth stage. The conductive electrons go through the priority conductive pathways and form a penetration current. So ρ sharply decreases with increasing d. When $d>$ 32 nm, Cr film has become a continuous structure and presents a metallic property. ρ decreases gradually until gets a steady value. Therefore, it indicates that the variation of resistivity with thickness is closely related to the film growth process and the change of structure.

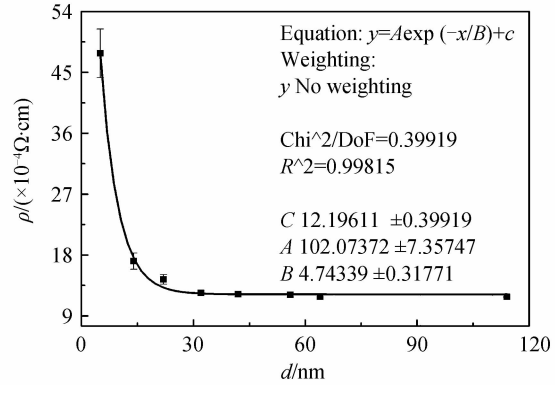

Fig. 6 Resistivity of the film as a function of thickness

It is assumed that ρ is the first order exponential decay with the increase of d as

$$\rho=A\exp(-d/B)+C \tag{4}$$

where A, B, and C are constants. The solid line in Fig. 6 is the simulated result by Eq. (4). As shown, the simulated result is in good agreement with the measured data. Moreover, $A=102\times10^{-4}\ \Omega\cdot$cm, $B=4.74$ nm, $C=12.2\times10^{-4}\ \Omega\cdot$cm.

3 Conclusion

1) Cr films with thickness ranging from 5 nm to 114 nm were deposited on quartz substrates by direct current magnetron sputtering. The films are

body-centered cubic crystalline structure. The mean grain size of the film increases gradually and the crystalline performance enhances with increasing film thickness.

2) When thickness is between 5 nm and 32 nm, film structure converts from the island growth stage to the network growth stage. Transmittance decreases sharply, reflectance and extinction coefficient increase rapidly as the increase of thickness. When thickness is larger than 32 nm, film growth is a continuous stage. As the increase of thickness, transmittance and reflectance at ultraviolet and visible spectral regions, refractive index, and extinction coefficient decrease slowly.

3) Resistivity presents the first order exponential decay with the increase of film thickness.

References

[1] BLOCH E, MISTELE D, BRENER R, *et al*. NiCr thin film resistor integration with InP technology[J]. *Semiconductor Science and Technology*, 2011, **26**(10): 105004.

[2] MILLER R A, HOLLAND H J. Crystallographic orientation of sputtered Cr films on glass and glass-ceramic substrates[J]. *Thin Solid Films*, 1997, **298**(1-2): 182-186.

[3] CHIANG K T K, WEI R H . Growth morphology and corrosion resistance of magnetron sputtered Cr films[J]. *Surface & Coatings Technology*, 2011, **206**(7): 1660-1665.

[4] LIN Wen-Jian Structure of an optical interference display unit: US, 6958847[P]. 2005-10-25.

[5] KIN T J, THIO T, EBBESEN T W, *et al*. Control of optical transmission through metals perforated with subwavelength hole arrays[J]. *Optics Letters*, 1999, **24**(4): 256-258.

[6] ZHANG Heng, ZHOU Yun, ZHOU Lei, *et al*. Fabrication of micro-grating structures by nanosecond laser ablation of chrome film on glass substrate[J]. *Acta Photonica Sinica*, 2009, **38**(2): 241-244.

[7] KULKARNI A K, CHANG L C. Electrical and structural characteristics of chromium thin films deposited on glass and alumina substrates[J]. *Thin Solid Film*, 1997, **301**(1-2): 17-22.

[8] SCHMIDT D, BOOSO B, HOFMANN T, *et al*. Generalized ellipsometry for monoclinic absorbing materials: determination of optical constants of Cr columnar thin films[J]. *Optics Letters*, 2009, **34**(7): 992-994.

[9] LI Hong-tao, JIANG Bai-ling, YANG Bo. Study on crystalline to amorphous structure transition of Cr coatings by magnetron sputtering[J]. *Applied Surface Science*, 2011, **258**(2): 935-939.

[10] URBAN III F K, BARTON D, TIWALD T. Numerical ellipsometry: Analysis of thin metal layers using n-k-d twisted curve methods with multiple incidence angles[J]. *Journal of Vacuum Science and Technology A*, 2010, **28**(4): 947-952.

[11] BESNARD A, MARTIN N, CARPENTIER L, *et al*. A theoretical model for the electrical properties of chromium thin films sputter deposited at oblique incidence[J]. *Journal of Physics D: Applied Physics*, 2011, **44**(21): 215301.

[12] FOROUGHI-ABARI A, XU C, CADIEN K C. The effect of argon pressure, residual oxygen and exposure to air on the electrical and microstructural properties of sputtered chromium thin films[J]. *Thin Solid Films*, 2012, **520**(6): 1762-1767.

[13] PEI Yu, LIN Li-mei, ZHENG Wei-feng, *et al*. Effect of passing electric current on the electrical and optical properties of ITO films in air[J]. *Surface Review and Letters*, 2009, **16**(6): 887-893.

[14] LAI Fa-chun, LIN Li-mei, HUANG Zhi-gao, *et al*. Effect of thickness on the structure, morphology and optical properties of sputter deposited Nb_2O_5 films[J]. *Applied Surface Science*, 2006, **253**(4): 1801-1805.

[15] LAI Fa-chun, LIN Li-mei, GAI Rong-quan, *et al*. Determination of optical constants and thicknesses of In_2O_3: Sn films from transmittance data[J]. *Thin Solid Films*, 2007, **515**(18): 7387-7392.

[16] MARK F. Optical properties of solids[M]. New York: Oxford University Press, 2001, 144.

[17] BRUCE C F, CLOTHIER W K. Optical properties of thin chromium films[J]. *JOSA*, 1974, **64**(6): 823-829.

[18] KAISER N. Review of the fundamentals of thin-film growth [J]. *Applied Optics*, 2002, **41**(16): 3053-3060.

磁控溅射制备铬薄膜的结构和光电学性质

林建平[1],林丽梅[2],关贵清[1],吴扬微[2],赖发春[2]

(1 宁德师范学院 物理与电气工程系,福建 宁德 352100)

(2 福建师范大学 物理系,福州 350108)

摘 要:用直流磁控溅射技术在石英基片上制备不同厚度(5 nm～114 nm之间)的铬膜.使用X射线衍射仪和分光光度计分别检测薄膜的结构和光学性质,利用德鲁特模型和薄膜的透射、反射光谱计算铬膜的厚度和光学常量,并采用Van der Pauw方法测量薄膜电学性质.结果表明:制备的铬薄膜为体心立方的多晶态,随着膜厚的增加,薄膜的结晶性能提高,晶粒尺寸增大;在可见光区域,当膜厚小于32 nm时,随着膜厚的增加,折射率快速减小,消光系数快速增大,当膜厚大于32 nm时,折射率和消光系数均缓慢减小并逐渐趋于稳定;薄膜电阻率随膜厚的增加为一次指数衰减.

关键词:磁控溅射;铬薄膜;结构;光学性质;电学性质